

## Sparse cryo-STEM tomography for biological samples

Antoine Cossa<sup>1</sup>, Véronique Arluison<sup>2</sup> and Sylvain Trépout<sup>3</sup>

<sup>1</sup>Université Paris-Saclay, Orsay, France, Ile-de-France, France, <sup>2</sup>Laboratoire Léon Brillouin LLB, CEA, CNRS UMR12, Université Paris Saclay, CEA Saclay, Gif-sur-Yvette, France, Ile-de-France, France, <sup>3</sup>Institut Curie, Université PSL, CNRS UMS2016, INSERM US43, Multimodal Imaging Center, 91400 Orsay, France, Ile-de-France, France

Cryo-electron tomography (Cryo-ET) enables to recover 3D information of cryo-fixed samples in a near-native state [Lučić *et al.* 2013] with a thickness up to ~250 nm [Aoyama *et al.* 2008]. Thicker samples (up to 1  $\mu\text{m}$ ) can be studied in scanning transmission electron microscopy (STEM), which consists in the raster scanning of a (sub-)nanometric convergent electron beam focused at the sample plane [Midgley & Weyland 2003][Pennycook 2012]. At equivalent electron dose, STEM induces less radiation damage to the sample than classical transmission electron microscopy (TEM) [Wolf *et al.* 2014] and is able to image micrometer thick cryo-fixed biological samples in 3D (see Fig. 1) [Trépout 2020]. However, in order to image thicker specimens or to reach higher magnifications we need to increase the dwell time or to sample the specimen more densely, respectively. This will inevitably increase the electron dose and the beam damage proportionally. The need to further reduce the electron dose emerges.

In this work, we present a sparse cryo-STET acquisition scheme. Instead of collecting a full frame for each tilt-angle, we collect only a fraction of the pixels. This permits to dramatically reduce the radiation dose received by the sample on each frame and across the full tilt-series. Multiple sparse data collection schemes have been previously investigated at our lab [Trépout 2019] (see Fig. 2). Before aligning the tilt-series, a pre-processing step is necessary to recover the missing information due to the data sparsity. Multiple inpainting methods are commonly used such as discrete cosine transform (DCT) [Garcia 2009], and shearlets transform [Kutyniok *et al.* 2014]. Then the 3D volume can be reconstructed using classical methods like weighted back-projection (WBP) [Radermacher 2006] implemented in IMOD [Kremer *et al.* 1996] or iterative algorithms such as simultaneous iterative reconstruction technique (SIRT) [Gilbert 1972] in Tomo3D [Agullero & Fernandez 2011].

To demonstrate the advantages of a sparse cryo-STET acquisition scheme, we applied our method on a sample that is too thick ( $> 1 \mu\text{m}$ ) to be studied using conventional TEM methods.

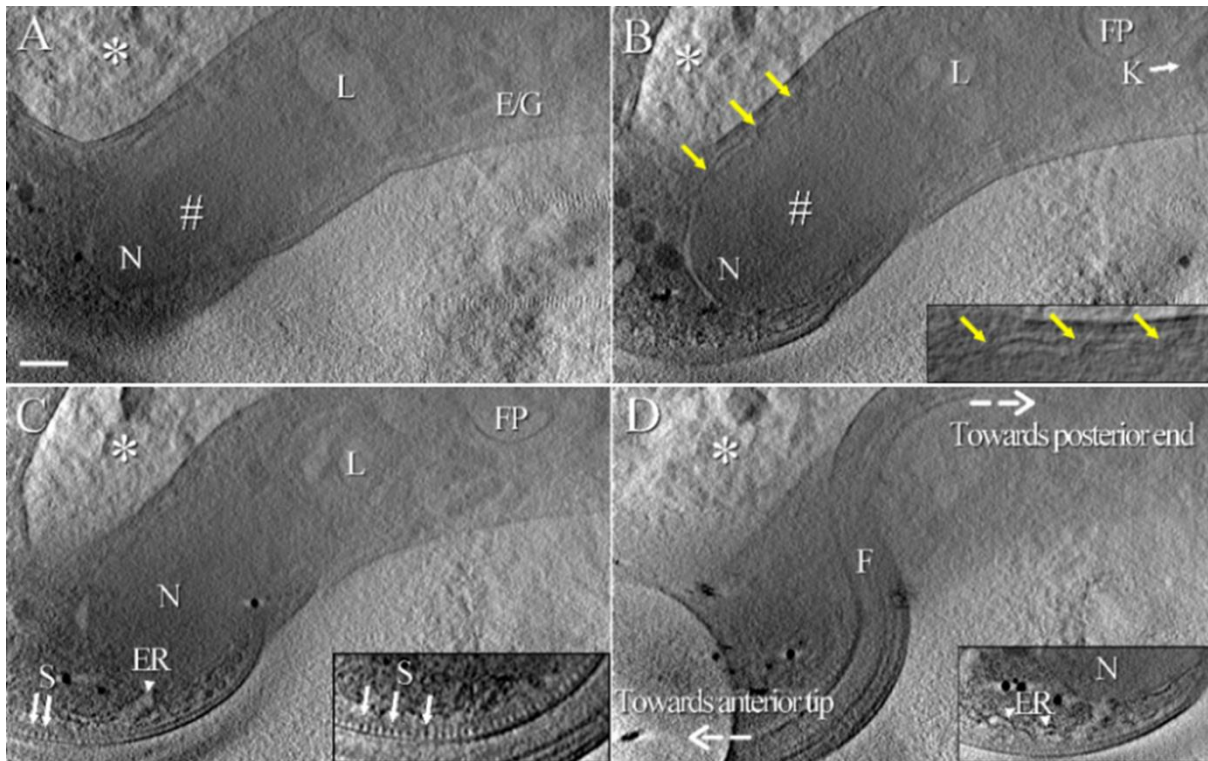


**Figure 1.** Figure 1. Ultrastructural organization of *T. brucei* observed in cryo-STET. 28 nm-thick tomographic slices showing intracellular structural elements of the cell. A) The nucleus (N), nucleolus (#), lysosome (L) and some endosomes and/or glycosomes (E/G) are visible. B) The kinetoplast (K), flagellar pocket (FP) and location of some nuclear pore complexes (yellow arrows) are visible. C) Regularly-spaced stick-like dark densities (S, arrows) correspond to the FAZ filament located next to the FAZ-associated reticulum (ER, arrowhead). The insert is an oriented slice in which sticks (S) are visible on a larger scale. D) The flagellum (F) coils on top of the cell body. The insert is an oriented slice showing the nucleus (N) and the FAZ-associated ER. The scale bar is 300 nm.

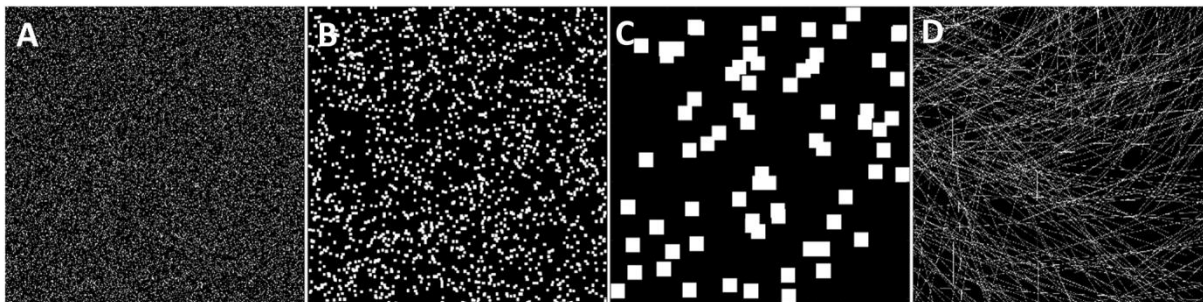


**Figure 2.** Figure 2. Multiples examples of sparse data collection. White pixels, representing 15% of the total number of pixels of the image, are arranged as A) individual pixels, B) 5x5 pixels patches, C) 25x25 pixels patches and D) oriented lines.

#### References

- [1] Lučić *et al.*, “Cryo-electron tomography: The challenge of doing structural biology in situ,” *J. Cell Biol.*, vol. 202, no. 3, pp. 407–419, 2013.
- [2] Aoyama *et al.*, “STEM tomography for thick biological specimens,” *Ultramicroscopy*, vol. 109, no. 1, pp. 70–80, 2008.

- [3] Midgley & Weyland, “3D electron microscopy in the physical sciences: the development of Z-contrast and EFTEM tomography,” p. 19, 2003.
- [4] Pennycook, “Seeing the atoms more clearly: STEM imaging from the Crewe era to today,” *Ultramicroscopy*, vol. 123, pp. 28–37, 2012.
- [5] Wolf *et al.*, “Cryo-scanning transmission electron tomography of vitrified cells,” *Nat. Methods*, vol. 11, no. 4, pp. 423–428, 2014.
- [6] Trépout, “In situ structural analysis of the flagellum attachment zone in *Trypanosoma brucei* using cryo-scanning transmission electron tomography,” *J. Struct. Biol. X*, vol. 4, p. 100033, 2020.
- [7] Trépout, “Tomographic Collection of Block-Based Sparse STEM Images: Practical Implementation and Impact on the Quality of the 3D Reconstructed Volume,” *Materials*, vol. 12, no. 14, p. 2281, 2019.
- [8] Garcia, “Robust smoothing of gridded data in one and higher dimensions with missing values,” *Comput. Stat. Data Anal.*, vol. 54, no. 4, pp. 1167–1178, 2010.
- [9] Kutyniok *et al.*, “Shearlets: Theory and Applications: Shearlets: Theory and Applications,” *GAMM-Mitteilungen*, vol. 37, no. 2, pp. 259–280, 2014.
- [10] Radermacher, “Weighted Back-projection Methods,” in *Electron Tomography*, J. Frank, Ed. New York, NY: Springer New York, 2006, pp. 245–273.
- [11] Kremer *et al.*, “Computer Visualization of Three-Dimensional Image Data Using IMOD,” *J. Struct. Biol.*, vol. 116, no. 1, pp. 71–76, 1996.
- [12] Gilbert, “Iterative methods for the three-dimensional reconstruction of an object from projections,” *J. Theor. Biol.*, vol. 36, no. 1, pp. 105–117, 1972.
- [13] Agulleiro & Fernandez, “Fast tomographic reconstruction on multicore computers,” *Bioinformatics*, vol. 27, no. 4, pp. 582–583, 2011.